Human Molecular Genetics, 2007, Vol. 16, No. 24 ***3059–3070***
doi:10.1093/hmg/ddm264
Advance Access published on September 13, 2007

Lack of fibulin-3 causes early aging and herniation, but not macular degeneration in mice

Precious J. McLaughlin[1], Benjamin Bakall[1], Jiwon Choi[5], Zhonglin Liu[2], Takako Sasaki[6], Elaine C. Davis[5], Alan D. Marmorstein[1,3] and Lihua Y. Marmorstein[1,4,*]

[1]Department of Ophthalmology and Vision Science, [2]Department of Radiology, [3]Optical Sciences Center and [4]Department of Physiology, University of Arizona, Tucson, AZ, USA, [5]Department of Anatomy and Cell Biology, McGill University, Montreal, Quebec, Canada and [6]Department of Biochemistry and Molecular Biology, Oregon Health and Science University, Portland, OR, USA

Received August 14, 2007; Revised and Accepted September 11, 2007

A mutation in the *EFEMP1* gene causes Malattia Leventinese, an inherited macular degenerative disease with strong similarities to age-related macular degeneration. *EFEMP1* encodes fibulin-3, an extracellular matrix protein of unknown function. To investigate its biological role, the murine *Efemp1* gene was inactivated through targeted disruption. *Efemp1*$^{-/-}$ mice exhibited reduced reproductivity, and displayed an early onset of aging-associated phenotypes including reduced lifespan, decreased body mass, lordokyphosis, reduced hair growth, and generalized fat, muscle and organ atrophy. However, these mice appeared to have normal wound healing ability. *Efemp1*$^{-/-}$ mice on a C57BL/6 genetic background developed multiple large hernias including inguinal hernias, pelvic prolapse and protrusions of the xiphoid process. In contrast, *Efemp1*$^{-/-}$ mice on a BALB/*c* background rarely had any forms of hernias, indicating the presence of modifiers for fibulin-3's function in different mouse strains. Histological analysis revealed a marked reduction of elastic fibers in fascia, a thin layer of connective tissue maintaining and protecting structures throughout the body. No apparent macular degeneration associated defects were found in *Efemp1*$^{-/-}$ mice, suggesting that loss of fibulin-3 function is not the mechanism by which the mutation in *EFEMP1* causes macular degeneration. These data demonstrate that fibulin-3 plays an important role in maintaining the integrity of fascia connective tissues and regulates aging.

INTRODUCTION

Fibulin-3 (also known as EFEMP1, S1-5, or FBNL) is a member of the fibulin family of extracellular matrix (ECM) proteins that share a common structure including tandem arrays of calcium-binding EGF domains and a characteristic carboxyl-terminal fibulin domain (1–4). Among the six known fibulins, fibulin-3 shares highest homology with fibulin-4 (also known as EFEMP2, MBP1, H411 or UPH1), and fibulin-5 (also known as DANCE or EVEC) (1–4). These three fibulins are deemed to be biologically important because mutations in their genes have been associated with several human diseases. A single mutation of an arginine to trypotophan (R345W) in *EFEMP1* causes Malattia Leventinese (ML), also known as Doyne honeycomb retinal dystrophy, an autosomal dominantly inherited macular degenerative disease (5). ML exhibits pathological features and clinical symptoms most similar to age-related macular degeneration (AMD), the leading cause of incurable blindness (6–8). A hallmark of both ML and AMD is the presence of sub-retinal pigment epithelium (RPE) deposits. Missense variations in fibulin-5 have been detected in a small number of patients with AMD (9). In addition, mutations in fibulin-4 and 5 have been found in patients with cutis laxa (10–12), a disease characterized by loose, redundant and inelastic skin. Fibulin-4 has also been found to be a target of autoimmunity in osteoarthritis patients (13). The broad spectrum of the diseases suggests that these fibulins have a wide range of functions and effects, though their precise functions and how defects in them cause diseases are not fully understood.

*To whom correspondence should be addressed at: Department of Ophthalmology and Vision Science, University of Arizona, 655 N Alvernon Way, Suite 108, Tucson, AZ 85711, USA. Tel: +1 5206260447; Fax: +1 5206260457; Email: lmarmorstein@eyes.arizona.edu

Several studies utilizing gene targeting in mice have provided insights into the functions of fibulin-4 and 5. *Fibulin-5* deficient mice exhibit disrupted and disorganized elastic fibers (14,15). We have reported that mice lacking fibulin-4 do not form intact elastic fibers and die perinatally due to severe vascular and lung defects (16). These studies indicate an essential role for fibulin-4 and 5 in elastic fiber formation. Based on their homology, it is reasonable then to speculate that fibulin-3 may also be important in elastic fiber biology. However, fibulin-3 displays little interaction with elastin, fibrillin-1, and other elastic fiber or basement membrane components, which do interact with fibulin-4 and 5 (17,18), and its presence does not compensate for loss of fibulin-4 or 5 function in mice. This suggests that fibulin-3 has distinct functions from those of fibulin-4 and 5.

EFEMP1 was originally cloned as S1-5 from senescent fibroblasts derived from a patient with Werner syndrome, a disease of premature aging (19). *EFEMP1* mRNA is overexpressed in Werner syndrome and senescent human fibroblasts (19). However, no mutations or other defects in the *EFEMP1* gene have been associated with Werner syndrome or other aging conditions. In normal tissues, fibulin-3 is highly expressed by epithelial and endothelial cells throughout the body (17,20,21), and is capable of inhibiting angiogenesis (22). In donor eyes from ML and AMD patients, fibulin-3 accumulates within the sub-RPE deposits and between the deposits and the RPE (23). The mutant fibulin-3 protein that causes ML is misfolded and accumulates inside cells overexpressing it (23). Thus, it has been speculated that the mutation in fibulin-3 may cause macular degeneration through damage to RPE cellular functions by protein misfolding and aggregation (23). However, it is highly possible that the mutation causes the disease through the impairment of a specific function that fibulin-3 may have in the eye.

In this study, we have generated *Efemp1* knockout mice and report the complex phenotype developed in these mice including early aging and strain specific herniation, but not macular degeneration. We found that fibulin-3 has a specific effect on the integrity of elastic fibers in fascia connective tissues that may explain the herniation phenotype. We also found that the genetic background of the mice greatly influences some phenotypes (e.g. herniation), suggesting the presence of modifier genes in different mouse strains that compensate for or suppress fibulin-3's effects.

RESULTS

Generation of *Efemp1*$^{-/-}$ mice

The mouse *Efemp1* gene was disrupted by replacing exons 4 and 5 with the neomycin-resistant gene sequence (Fig. 1A) through homologous recombination (Fig. 1B). This resulted in the complete ablation of *Efemp1*. Reverse transcription–polymerase chain reaction (RT–PCR) (Fig. 1C) and western blot analysis (Fig. 1D) demonstrated that there was no transcript or protein present in the homozygous mice. We maintained the mice in this study on two mixed background, 129Sv/J-BALB/c or 129Sv/J-C57BL/6. The BALB/c mixed strain had an albino or chinchilla coat color, and the C57BL/6 mixed strain had a brown or black coat color. Both

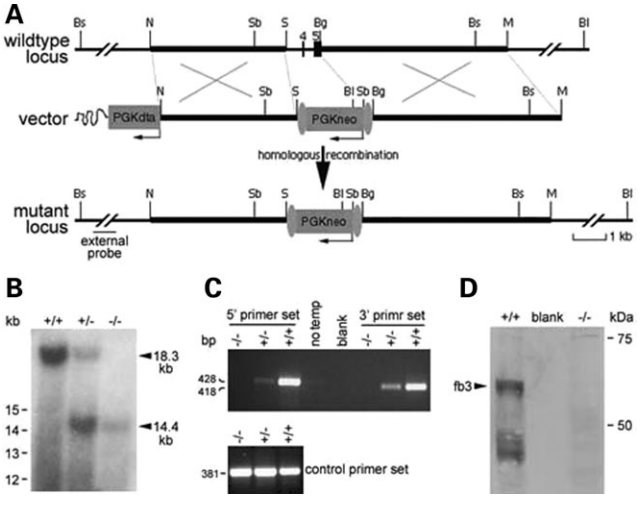

Figure 1. Targeting strategy to generate *Efemp1* knockout mice. (**A**) Schematic diagram of the wild-type locus, targeting vector and mutant locus. Thick lines represent homologous 5′ and 3′ arms. Numbered solid boxes depict *Efemp1* exons. Bs, BsrGI; N, NheI; Sb, SbfI; S, SalI; Bg, BglII; M, MfeI; Bl, BlpI. (**B**) Southern blot analysis of mouse genomic DNA. The 18.3-kb wild-type band and 14.4 kb mutant band were detected by the external probe/BsrGI and BlpI digestion. (**C**) RT–PCR analysis of mouse RNA. No PCR product was detected for homozygous mice using either a 5′ or 3′ primer set (upper panel), indicating the absence of *Efemp1* mRNA in these mice. In the control (lower panel), PCR products were detected for all mice using a primer set for *fibulin-4*. (**D**) Western blot of lung extracts from wild-type and *Efemp1*$^{-/-}$ mice using an antibody against mouse fibulin-3. A band at ~63 kDa was detected in the wild-type extract (+/+ lane), but not in the *Efemp1*$^{-/-}$ extract (−/− lane). The lower band in the +/+ lane may be partially degraded fibulin-3 or a splice variant of fibulin-3. fb3, fibulin-3.

Efemp1$^{+/-}$ and *Efemp1*$^{-/-}$ mice were born with a Mendelian ratio and showed no gross differences from their wild-type littermates at birth. Therefore, fibulin-3 was not required for mouse early survival.

Herniation in *Efemp1*$^{-/-}$ mice with C57BL/6 background

When mice grew to 2 months of age or older, we started to notice that visually discernable bulges or protrusions developed at several sites in both male and female pigmented *Efemp1*$^{-/-}$ mice that had been bred against a C57BL/6 genetic background. There were lateral bulges (either unilateral or bilateral) near hind legs, rear bulges with or without rectal prolapse in anorectal area, or protrusions in the chest area.

Autopsy of mice sacrificed at varying ages revealed that the lateral bulges (Fig. 2A and B) consisted of fat tissue and/or other abdominal contents (Fig. 2C and D). In heavier mice with abundant fat tissues in the abdominal cavity, fat bodies were herniated out first (Fig. 2C), but in mice with little abdominal fat, hernias contained other abdominal contents such as intestines (Fig. 2D). The content of hernias could be freely moved around and back and forth into the abdominal cavity. Although some hernias appeared to originate on the backs of the mice (Fig. 2C and D), we found that all of them herniated out from the myopectineal orifice, a small spot in the inguinal area where the abdominal wall is devoid of muscle and contains only transverse fascia, a thin layer of

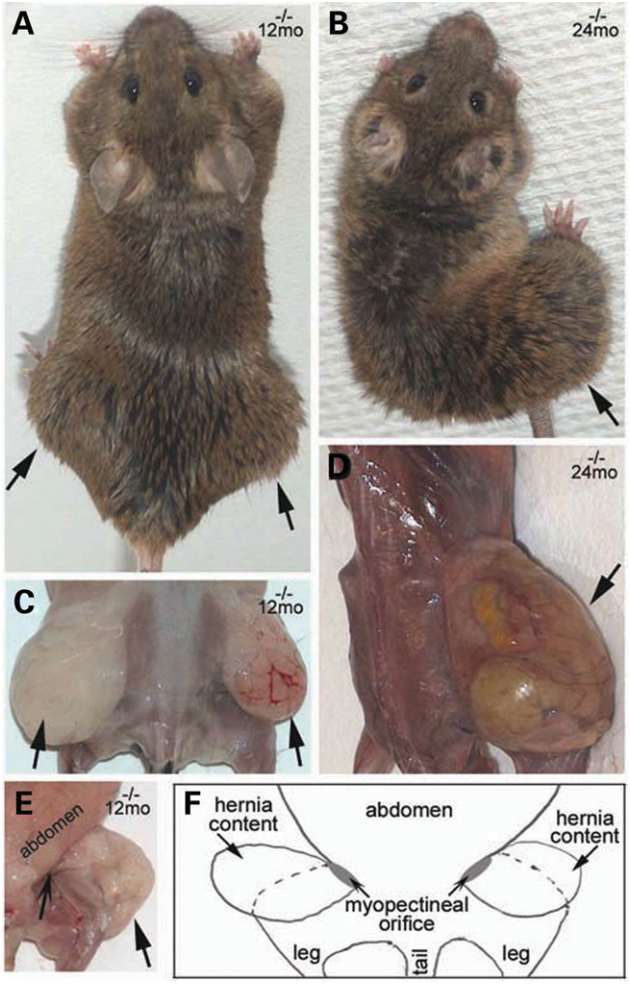

Figure 2. Direct inguinal hernias in *Efemp1*$^{-/-}$ mice on the C57BL/6 genetic background. (**A**) A 12 month-old *Efemp1*$^{-/-}$ mouse. Note the bilateral bulges (arrows) near the hind legs. (**B**) A 24 month-old *Efemp1*$^{-/-}$ mouse. Note the large bulge (arrow) near the right hind leg. (**C**) Dissection of the mouse in (A) revealed that the lateral bulges contain fat tissues (arrows). (**D**) The large bulge of the mouse in (B) contained abdominal contents such as intestines (arrow). (**E**) Anterior view of the mouse in (C) showing that the fat bulge (arrow) was a hernia from the inguinal area (concave arrow). (**F**) A diagram to illustrate the location of the myopectineal orifice (concave arrows), the site of herniation.

aponeurotic connective tissue (Fig. 2E and F). Thus, they are direct inguinal hernias.

Anorectal bulges in *Efemp1*$^{-/-}$ mice were different in males from females. In males (Fig. 3A), they were often unilateral or asymmetrical, especially when they first became noticeable and were small in size, and they were not accompanied by rectal prolapse as frequently as in females. On dissection, the smaller bulges usually contained only fat tissues (Fig. 3B), and the larger bulges contained both fat and abdominal contents. These contents appeared to herniate out of the abdominal cavity at the myopectineal orifice through the external inguinal ring of the inguinal canal and together with the spermatic cord down to the scrotum (Fig. 3B). When the hernias became more severe and larger or when they occurred bilaterally, the entire area was occupied. Thus, in male *Efemp1*$^{-/-}$ mice, the rear bulges

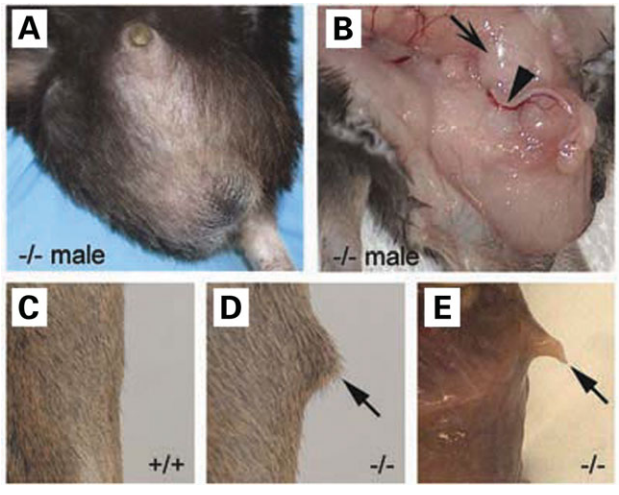

Figure 3. Indirect inguinal hernias and xiphoid protrusions in *Efemp1*$^{-/-}$ mice on the C57BL/6 genetic background. (**A**) A 12 month-old male *Efemp1*$^{-/-}$ mouse showing a large bulge at the anorectal area. (**B**) Partial dissection of the rear bulge in a 3 month-old male *Efemp1*$^{-/-}$ mouse. Note that the bulge contained fat tissue herniated out of the abdominal cavity at the same site (arrow) where the spermatic cord (arrowhead) leaves the abdominal cavity. (**C**–**E**) Lateral view of the chest area of a 12 month-old wild-type mouse showing no protrusions on the chest (C) or a 12 month-old *Efemp1*$^{-/-}$ mouse showing a protrusion (arrow) on the chest (D), and dissection of the mouse (E) showed that the protrusion was the xiphoid process (arrow). +/+, wild-type; −/−, *Efemp1*$^{-/-}$.

were indirect inguinal hernias. In humans, indirect inguinal hernias are much more common in men than women owing to the much larger inguinal canals in men. In female *Efemp1*$^{-/-}$ mice, the rear bulges contained pelvic organs such as uterus, bladder, and rectum (data not shown). Thus, they were the results of pelvic organ prolapse. The vesical ligaments of the pelvic fascia covering and supporting pelvic organs appeared to be disrupted in these mice. These ligaments are thin layers of fascia connective tissues similar to the transverse fascia membranes covering the myopectineal orifice.

Autopsy revealed that the protrusion (Fig. 3D) at the base of the thorax in *Efemp1*$^{-/-}$ mice was xiphoid process (Fig. 3E), a cartilaginous extension of the lower part of the sternum. The abdominal cavity wall covering this cartilage is composed of fascia membranes at the tip of the linea alba, a thin layer of aponeurotic connective tissue, and a layer of superficial fascia. This is a weak point where some epigastric hernias are found in humans. In mice the xiphoid process is proportionally larger than in humans. Both male and female *Efemp1*$^{-/-}$ mice developed xiphoid process protrusions.

One hundred percent of *Efemp1*$^{-/-}$ mice on the C57BL/6 background developed at least one form of these hernias or protrusions during their lifespan, and frequently an individual mouse had two or more forms of hernias. The time of onset varied, ranging from 2 months to over 1 year of age. The degree of severity also varied, but increased progressively with age. Both male and female mice developed hernias. We did not find significant differences in severity or the onset time of the hernias between male and female mice. None of the wild-type or *Efemp1*$^{+/-}$ littermates of *Efemp1*$^{-/-}$ mice developed any hernias or protrusions (Fig. 3C).

Interestingly, we did not find any direct inguinal hernias or xiphoid protrusions in *Efemp1*$^{-/-}$ mice on the BALB/c genetic background with albino or chinchilla coat color. Occasionally we found rear bulges associated with albino *Efemp1*$^{-/-}$ mice with an advanced age (over 1 year old). The differences in hernia phenotypes between C57BL/6 and BALB/c strains suggest that modifier(s) exist for fibulin-3's effect in different strains.

Reduced elastic fibers in fascia of *Efemp1*$^{-/-}$ mice

There is a similarity among the sites of hernias or protrusions in *Efemp1*$^{-/-}$ mice. Transverse fascia at the myopectineal orifice, linea alba, or the vesical ligaments of the pelvic fascia were found to be disrupted at the sites. These structures are all fascia membranes. Fascia is a thin layer of connective tissue that is present throughout the body. It surrounds muscles, bones, joints and organs, providing support, protection and giving structure to the body (24). Fascia is generally classified into superficial fascia located directly under the skin, deep fascia beneath the superficial fascia, and visceral fascia associated with the cavities of the body (24). We sampled fascia membranes from a number of sites in wild-type and *Efemp1*$^{-/-}$ mice on either a C57BL/6 or BALB/c background. Histological analysis revealed that all fascia membranes contained prominent collagen fibers in both wild-type and *Efemp1*$^{-/-}$ mice (data not shown). In wild-type mice, elastic fibers were prominent (Fig. 4A and C) and were more abundant in visceral than superficial fascia. However, fascia membranes from the *Efemp1*$^{-/-}$ mice showed a marked reduction in elastic fiber networks (Fig. 4B and D). Interestingly, the reduction was more severe in C57BL/6 than BALB/c *Efemp1*$^{-/-}$ mice. There were faint, fine elastic fibers visible in BALB/c *Efemp1*$^{-/-}$ membranes (Fig. 4D), but a near absence of elastic fibers in C57BL/6 *Efemp1*$^{-/-}$ membranes (Fig. 4B).

To determine whether elastic fibers in other tissues were affected and whether the ultrastructure of elastic fibers was altered in *Efemp1*$^{-/-}$ mice, we performed a light and electron microscopic study on aorta, lung and skin. By light microscopy, elastin staining revealed no obvious differences in the elastic lamina of aorta and elastic fibers in lung. However, a slight reduction in the elastic fiber network in the skin was observed in *Efemp1*$^{-/-}$ mice (data not shown). This reduction was similar in C57BL/6 and BALB/c mice. The two main components of elastic fibers, elastin and microfibrils, are easily distinguished by electron microscopy. At 3 months of age, the dermal elastic fibers in wild-type mice consisted of a relatively solid core of elastin with microfibrils surrounding, and embedded within, the elastin (Fig. 5A). In contrast, the elastin appeared considerably more fragmented, with the microfibrils being much more visible in elastic fibers from *Efemp1*$^{-/-}$ mouse skin (Fig. 5B). By 8 months of age, the dermal elastic fibers in wild-type and *Efemp1*$^{-/-}$ mice appeared similar, both being somewhat mottled in appearance (Fig. 5C and D). No discernible ultrastructural differences were found in the elastic laminae of aorta and elastic fibers in lung of *Efemp1*$^{-/-}$ mice (data not shown). These results demonstrate that a lack of fibulin-3 causes a severe reduction in elastic fiber content in fascia, but only subtle or no effect on elastic fibers in other tissues we examined.

Efemp1$^{-/-}$ mice exhibit reduced reproductivity

Regardless of genetic background, we observed that *Efemp1*$^{-/-}$ mice were either sterile or produced very few pups and stopped breeding quickly. We monitored breeding pairs of wild-type or *Efemp1*$^{+/-}$ mice and breeding pairs containing one *Efemp1*$^{-/-}$ mouse and one wild-type or *Efemp1*$^{+/-}$ mouse. While wild-type or *Efemp1*$^{+/-}$ mice had as many as 17 litters during their life time and as many as 16 pups in an individual litter, breeding pairs containing a *fibulin-3*$^{-/-}$ mouse had a maximum of four litters and a maximum of five pups in any individual litter (Supplementary Material, Table S1). Only one female *Efemp1*$^{+/-}$ mouse we monitored never produced any offspring, but 41% of the *Efemp1*$^{-/-}$ mice monitored (11 out of 27) were sterile. The wild-type or *Efemp1*$^{+/-}$ mice produced a median of 11 litters and seven pups in an individual litter. The *Efemp1*$^{-/-}$ mice that were not sterile produced a median of two litters and two pups in an individual litter (Supplementary Material, Table S1). The findings were similar for both male and female *Efemp1*$^{-/-}$ mice with either C57BL/6 or BALB/c background. These data indicated a markedly reduced reproductivity of *Efemp1*$^{-/-}$ mice.

Efemp1$^{-/-}$ mice have reduced lifespan and display early aging phenotypes

The *Efemp1*$^{-/-}$ mice died at a much younger age than their wild-type littermates. The median lifespan of the *Efemp1*$^{-/-}$ mice was 93 weeks compared with 115 weeks for their wild-type littermates, and the maximal lifespan of the *Efemp1*$^{-/-}$ mice was 121 weeks compared with 170 weeks for the wild-type mice (Supplementary Material, Table S2). Thus, the lifespan of *Efemp1*$^{-/-}$ mice was significantly shorter than wild-type mice. A precise cause of death was difficult to determine. Although some of the C57BL/6 *Efemp1*$^{-/-}$ mice might have died from hernia complications, postmortem examination did not reveal any obvious vital defects in the *Efemp1*$^{-/-}$ mice, and this shortened lifespan was similar for all the *Efemp1*$^{-/-}$ mice regardless of genetic background. During the first 10 months of age, other than hernias or protrusions in the C57BL/6 *Efemp1*$^{-/-}$ mice, the only morphological difference noted was that the skin of some *Efemp1*$^{-/-}$ mice (regardless of the genetic background) was looser than their wild-type littermates when they were several months old (data not shown). This was more visually distinguishable in males than females. While this condition was not dramatic, the gross appearance of some *Efemp1*$^{-/-}$ mice became obviously different from their wild-type littermates by 12 months of age, and the difference became highly consistent in all the *Efemp1*$^{-/-}$ mice by 18 months of age. They exhibited a host of signs of early aging including an absence of vigor, loss of hair glossiness, coarse hair, hair thinning on the back, reduced body size, lordokyphosis and frequent periophthalmic lesions (Fig. 6A and C; Supplementary Material, Table S2).

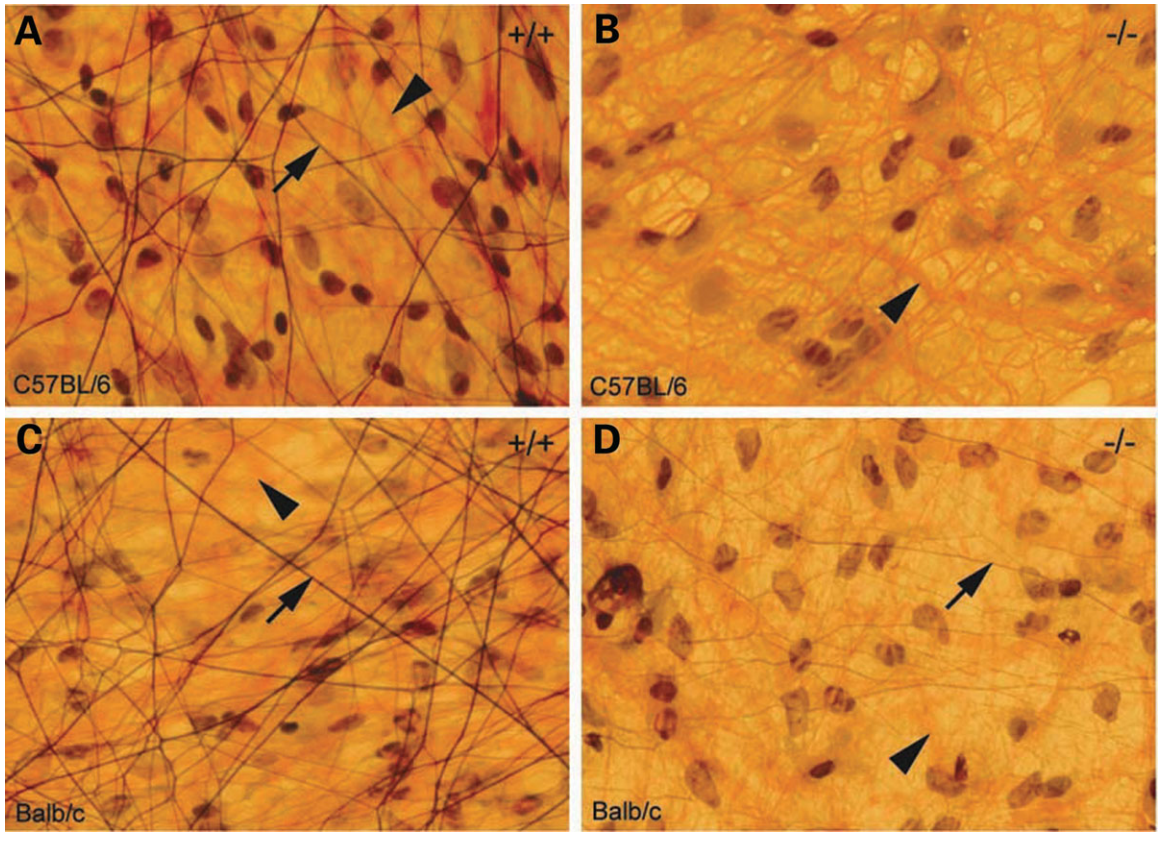

Figure 4. Reduced elastic fibers in fascia of *Efemp1*$^{-/-}$ mice. Spread preparations of visceral fascia from 12 month-old mice were stained for elastin. (**A**) Fascia from a wild-type mouse with C57BL/6 background. Note the prominent elastic fiber network (black; arrow) and the collagen fiber network (red; arrowhead). (**B**) Fascia from an *Efemp1*$^{-/-}$ mouse with C57BL/6 background. Note the absence of elastic fibers and the prominent collagen fibers (red, arrowhead). (**C**) Fascia from a wild-type mouse with BALB/c background showing prominent elastic fiber (black; arrow) and collagen fiber (red; arrowhead) networks. (**D**) Fascia from an *Efemp1*$^{-/-}$ mouse with BALB/c background. Note the presence of a faint, fine elastic fiber network (black; arrow) and a prominent collagen fiber network (red; arrowhead).

Weighing the mice at 18–24 months of age confirmed significant reductions in the body mass of *Efemp1*$^{-/-}$ mice compared with their age-matched wild-type littermates (Fig. 6F). Whole body X-ray analysis showed a severely curved spine and reduced bone density in *Efemp1*$^{-/-}$ mice indicating pronounced lordokyphosis and osteoporosis (Fig. 6B and E). Autopsy of *Efemp1*$^{-/-}$ mice sacrificed at older ages demonstrated clear, visible reductions in adipose tissues and muscle mass in comparison to wild-type littermates. Isolated calf muscle weights from 24 months old *Efemp1*$^{-/-}$ and wild-type mice indicated an over 30% reduction in the mean muscle mass in *Efemp1*$^{-/-}$ mice (Fig. 6J). Dissection and histopathological examination revealed atrophic and degenerating internal organs including spleen, liver, kidney, testes and uterus in 18–24 month old *Efemp1*$^{-/-}$ mice (Fig. 6D). The mean weight of internal organs such as spleen, liver and kidney from *Efemp1*$^{-/-}$ mice was significantly ($P<0.05$) reduced compared to wild-type mice (Fig. 6G–I). Both males and females showed comparable reductions in body weight and organ masses. These results are consistent with human aging. Reductions in body, liver, spleen and kidney masses are a normal consequence of aging in humans over 60 years of age (25).

Histological analysis of skin sections revealed significant differences in the thickness of subcutaneous adipose of aged (24 months old) wild-type and *Efemp1*$^{-/-}$ mice (Fig. 7C and D), but no obvious differences were seen in young (3 months old) mice (Fig. 7A and B). While a substantial layer of subcutaneous adipose was present in the skin of old wild-type mice (Fig. 7C), virtually no subcutaneous adipose was observed in the skin of old *Efemp1*$^{-/-}$ mice (Fig. 7D). Although reduced dermal thickness is associated with aging in humans (26), we did not find significant differences in dermal thickness between wild-type and *Efemp1*$^{-/-}$ mice (Fig. 7C and D).

Hair growth declines as a function of age in mice (27). We observed hair thinning on the nucha and dorsum of older *Efemp1*$^{-/-}$ mice. To test whether *Efemp1*$^{-/-}$ mice have reduced ability to regrow hair, we performed hair regrowth assays with two age groups of mice: relatively young (5–10 months old) and relatively old (19–21 months old). In each group, age-matched littermates of wild-type and *Efemp1*$^{-/-}$ mice were used. After shaving a dorsal segment of skin and measuring the amount of hair growth after 25 days, we found no differences in hair growth in younger wild-type and *Efemp1*$^{-/-}$ mice. Hair completely regrew within 25

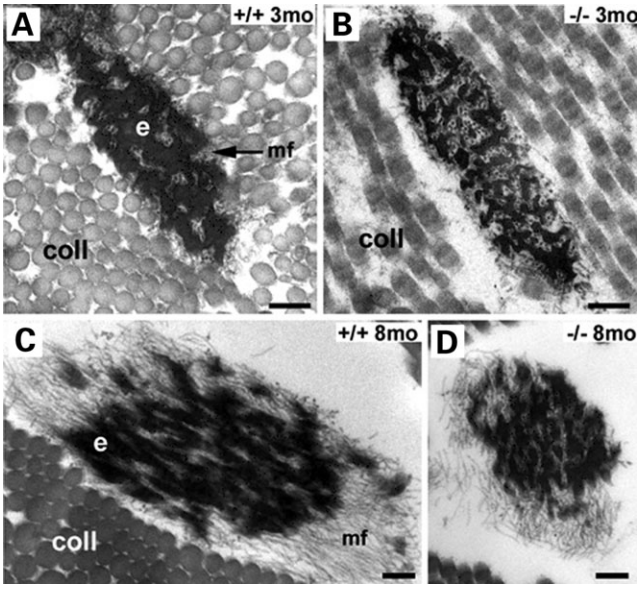

Figure 5. Electron microscopy of dermal elastic fibers in wild-type and *Efemp1*$^{-/-}$ mice. Cross-sections of elastic fibers from wild-type (**A**) and *Efemp1*$^{-/-}$ (**B**) mice at 3 months of age. Note that the elastin core (e) of the elastic fiber is more fragmented in the *Efemp1*$^{-/-}$ dermis resulting in the microfibrils (mf) being more evident. Dermal collagen fibers run multidirectional and are not always oriented in the same way as dermal elastic fibers. Other than differences in orientation, collagen fibers appeared to be similar in both wild-type and *Efemp1*$^{-/-}$ mice. (**C** and **D**) Oblique sections of elastic fibers from wild-type (C) and the *Efemp1*$^{-/-}$ (D) mice at 8 months of age. No obvious differences in elastic fiber ultrastructure can be seen at this age between the wild-type and *Efemp1*$^{-/-}$ mice. coll, collagen; scale bar: 200 nm.

days. However, older *Efemp1*$^{-/-}$ mice only had very limited hair regrowth 25 days after shaving (Fig. 8B and D), while the wild-type mice had complete hair regrowth (Fig. 8A and C). The mean hair regrowth was reduced by >50% in *Efemp1*$^{-/-}$ mice compared to their wild-type littermates (Fig. 8E).

Some aging features such as hair graying, skin ulceration or cataracts were not increased in frequency in the older *Efemp1*$^{-/-}$ mice. There were no obvious differences in lungs, heart and intestines in the older wild-type and *Efemp1*$^{-/-}$ mice. Blood cell counts were similar in wild-type and *Efemp1*$^{-/-}$ mice (data not shown). Thus, the older *Efemp1*$^{-/-}$ mice display an early onset of most, but not all, phenotypes associated with aging.

Normal wound healing in *Efemp1*$^{-/-}$ mice

One function of age in both mice and humans is a reduced ability to deal with stresses such as wound healing (28). To test this capacity, we performed wound-healing assays with both young (3 months) and old (24 months) mice. Wounds were induced and monitored over a period of 10 days for closure before sacrifice. As shown in Fig. 9, neither young nor old *Efemp1*$^{-/-}$ mice showed any significant differences in wound sizes from their age-matched wild-type controls. Thus, *Efemp1*$^{-/-}$ mice appeared to have normal wound healing capability.

No apparent macular degeneration-associated defects in *Efemp1*$^{-/-}$ mice

Since a mutation in the *EFEMP1* gene causes ML, we investigated whether *Efemp1*$^{-/-}$ mice had any eye defects associated with macular degeneration. The pathogenic site in human ML patients is at the level of Bruch's membrane and the RPE. Immunofluorescence staining confirmed that the fibulin-3 protein was present in Bruch's membrane (Fig. 10B) in wild-type (Fig. 10A and B), but not *Efemp1*$^{-/-}$ mice (Fig. 10C and D). Bruch's membrane is a layered membrane structure containing the basement membrane of the RPE, collagen and elastic fiber layers and the basement membrane of the choroidal capillary endothelial cells (29). These layers are very thin and are not distinguishable under the light microscope. Electron microscopy showed that the elastic fiber layer of Bruch's membrane appeared to be more discontinuous and less homogeneous in *Efemp1*$^{-/-}$ mice than wild-type mice (Fig. 10E and F). But overall, the layered structures of Bruch's membrane were similar in wild-type and *Efemp1*$^{-/-}$ mice. The RPE basal infoldings appeared less convoluted and more compacted in *Efemp1*$^{-/-}$ mice than that in wild-type mice (Fig. 10E and F). No obvious difference was observed in other parts of the RPE and the retina in *Efemp1*$^{-/-}$ mice. Importantly, we did not observe any sub-RPE deposits, the hallmark of macular degeneration, in *Efemp1*$^{-/-}$ mice, even at advanced ages (over 18 months old). It is unlikely that anatomical differences between human and mouse retinas (30) account for the lack of macular degeneration-associated defects in *Efemp1*$^{-/-}$ mice, since sub-RPE deposits are prominent in a knock-in mouse model harboring the R345W mutation in the *Efemp1* gene (31,32). This result suggests that macular degeneration due to mutation of *Efemp1* is not the result of a loss of function.

DISCUSSION

The *Efemp1*$^{-/-}$ mice generated in this study exhibit several seemingly unrelated phenotypes including herniation and early aging. We found that the herniation was due to disruption of fascia membranes in *Efemp1*$^{-/-}$ mice. Although the precise cause of early aging is difficult to determine, we hypothesize that a weakening or disruption in fascia contributes to the early aging in *Efemp1*$^{-/-}$ mice. Loose skin is one characteristic of early aging and *Efemp1*$^{-/-}$ mice exhibit loose skin as early as 3 months of age. It is highly probable that the loose skin is the result of a weakening or disruption in the superficial fascia, which connects the skin to the body and serves as a protective padding to cushion the subcutis. Defects in fascia could also cause the other early aging symptoms observed in *Efemp1*$^{-/-}$ mice. Fascia is extensive and associated with virtually every part of the body. Not only do fascia membranes connect skin to the body, they also interpenetrate and envelop the muscles, bones, cartilage, nerves and blood vessels, and suspend organs within their cavities. Fascia serves diverse functions maintaining and connecting structures, providing a passageway for lymph, nerve and blood vessels, storing fat and water, and protecting the internal structures from injury (24). A disruption in fascia may not result in an abrupt dysfunction of any organ, but it can lead

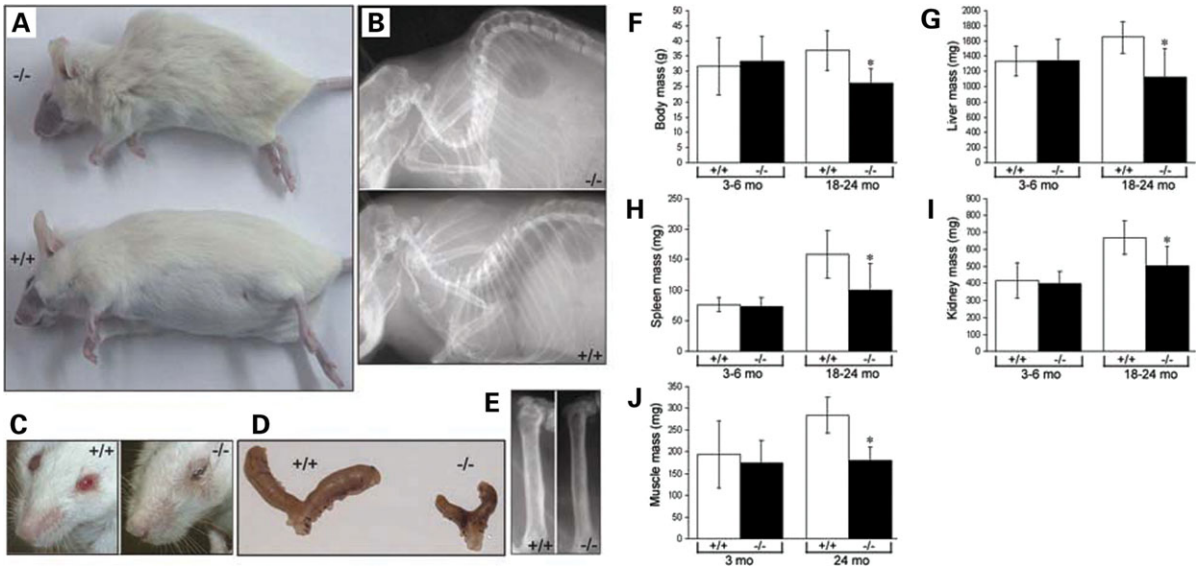

Figure 6. Age-associated phenotypes in *Efemp1*$^{-/-}$ mice. (**A**) Gross appearance of an 18 month-old female *Efemp1*$^{-/-}$ mouse (−/−) in comparison with its wild-type female littermate (+/+). Note the small body size and coarse hair of the *Efemp1*$^{-/-}$ mouse. (**B**) Whole body X-ray images (lateral) of 18 month-old *Efemp1*$^{-/-}$ (−/−) and wild-type (+/+) mice showing the curvature of the spine. Note the severely curved spine of the *Efemp1*$^{-/-}$ mouse. (**C**) Periophthalmic lesions in an 18 month-old *Efemp1*$^{-/-}$ mouse (−/−), but not in the wild-type littermate (+/+) co-caged with it. (**D**) The uterus of an 18 month-old *Efemp1*$^{-/-}$ mouse (−/−) was small and atrophic compared to that of its wild-type littermate (+/+). (**E**) X-ray images of femurs showing reduced bone density in a 18 month-old *Efemp1*$^{-/-}$ (−/−) mouse compared to that of an age-matched wild-type control (+/+). (**F**–**J**) Comparisons of mean wild-type (+/+; white columns) and *Efemp1*$^{-/-}$ (−/−; black columns) body (F), liver (G), spleen (H), kidney (I) and muscle (J) masses. Note the significant mass reductions in older (18–24 months) *Efemp1*$^{-/-}$ mice. Data are mean ± SD, $n=5$ for each genotype at each age. *$P<0.05$, compared to the wild-type by *t*-test.

to displacement and loss of protection and support. Ultimately, the integrity of the body is compromised. Changes in shape, damage due to trauma, altered patterns of blood and lymph circulation, and changed access to local fat supplies could also result in a gradual deterioration of organ functions that closely resembles aging.

The phenotypic data from *Efemp1*$^{-/-}$ mice provide important clues to fibulin-3's function. The principle defect observed in *Efemp1*$^{-/-}$ fascia was a dramatic reduction of elastic fiber networks. To date, the only protein reported to interact strongly with fibulin-3 is tissue inhibitor of metalloproteinase-3 (TIMP-3), an endogenous inhibitor of matrix metalloproteinases (MMPs) (33). Thus, it is possible that fibulin-3 functions to protect elastic fibers from degradation by ECM enzymes. We hypothesize that fibulin-3 is an ECM enzyme antagonist that augments the inhibitory activity of TIMP-3 or antagonize MMPs or other ECM enzymes directly. The tissue specificity may be dictated by the location of fibulin-3 or the enzymes. Fibulin-3 is highly expressed by endothelial and epithelial cells and is particularly abundant in small blood vessels (17,20,21). Since fascia serves as a passageway for and contains large numbers of lymph and small blood vessels, a lack of fibulin-3 may greatly impact the integrity of the organs they connect by altering the flow of blood and lymph. Alternatively, fibulin-3 may also have subtle but wide effects on multiple tissues, with its effects being particularly evident only in the thin layers of the fascia membranes. The enzyme(s) antagonized by fibulin-3 may have specific effects on ECM remodeling in tissues beyond fascia. For example, the enzyme(s) may normally be involved in bone remodeling but not wound healing. This could explain why *Efemp1*$^{-/-}$ mice have reduced bone density, but normal wound healing ability. Although our data did not reveal obvious differences in collagen fibers or other ECM components between wild-type and *Efemp1*$^{-/-}$ mice, we cannot rule out the possibility that other defects do exist but were undetected by our methods of analysis.

It is interesting that herniation is predominantly manifested in *Efemp1*$^{-/-}$ mice on the C57BL/6 but not BALB/c background. This suggests a lack of a compensatory gene(s) for fibulin-3's function or the presence of enhancing gene(s) for herniation specifically in C57BL/6 strains. Although it is well known that genetic background can greatly influence the phenotypes of genetically engineered mice, it is often difficult to pin point the modifier for any specific features. In comparison with C57Bl/6 mice, BALB/c mice have significantly higher levels of TIMP-1 and MMP-3 than C57BL/6 mice in response to certain pathological conditions (34). If fibulin-3 functions as an ECM enzyme antagonist, a higher level of TIMPs or other protective MMPs in response to the lack of fibulin-3 may contribute to the less severe herniation phenotype in *Efemp1*$^{-/-}$ mice on the BALB/c background. Correlating with this theory, our histological analysis found that elastic fibers were virtually absent in fascia of C57BL/6 *Efemp1*$^{-/-}$ mice, but were significantly reduced, though present in fascia of BALB/c *Efemp1*$^{-/-}$ mice.

Fibulin-3 shares ∼50% amino acid identity, and is nearly identical in its structural organization to fibulin-4 and 5 (1,2,4). Previous studies have shown that both fibulin-4 and 5 play essential roles in elastic fiber formation (14–16). Our findings, however, suggest that the function of fibulin-3 in relation to elastic fibers is much less critical than that of

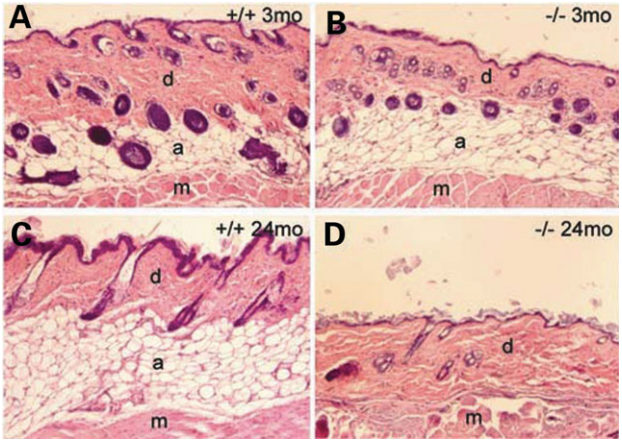

Figure 7. Reduced subcutaneous adipose in older *Efemp1*$^{-/-}$ mice. H&E stained sections of dorsal skin from a 3 month-old wild-type mouse (**A**), a 3 month-old *Efemp1*$^{-/-}$ mouse (**B**), a 24 month-old wild-type mouse (**C**), and a 24 month-old *Efemp1*$^{-/-}$ mouse (**D**). Note the near absence of subcutaneous adipose in the 24 month-old *Efemp1*$^{-/-}$ mouse (D). d, dermis; a, subcutaneous adipose tissue; m, muscle.

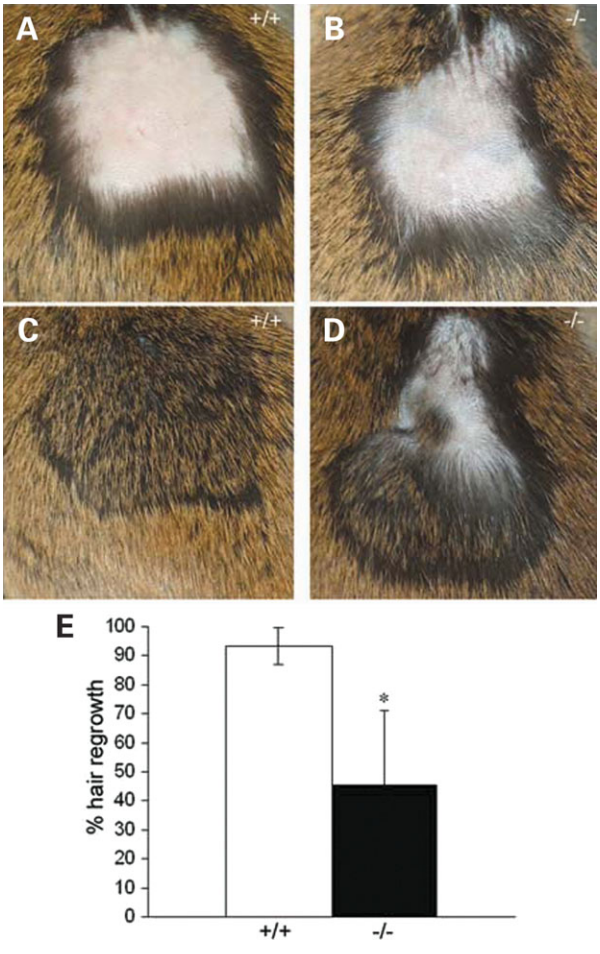

Figure 8. Reduced hair regrowth in older *Efemp1*$^{-/-}$ mice. (**A**) A shaved area in a 19 month-old wild-type mouse right after shaving. (**B**) A shaved area in a 19 month-old *Efemp1*$^{-/-}$ mouse right after shaving. (**C**) The same area as in (A) 25 days after shaving. (**D**) The same area as in (B) 25 days after shaving. (**E**) Mean hair regrowth scored with a transparent grid screen in 19–21 month-old *Efemp1*$^{-/-}$ (−/−; black column) mice ($n = 6$) and their age-matched wild-type littermate controls (+/+; white column) ($n = 8$). Data are mean ± SD. $^{*}P < 0.05$, compared to the wild-type by *t*-test.

fibulin-4 or 5. Elastic fibers in tissues other than fascia are only mildly affected or unaffected, and no obvious defects were identified in elastogenic organs such as blood vessels and lung in *Efemp1*$^{-/-}$ mice. In contrast, *fibulin-4*$^{-/-}$ mice have severe vascular and lung defects and exhibit no intact elastic fibers in any tissue (16). *Fibulin-5*$^{-/-}$ mice exhibit loose skin, emphysematous lungs, a stiff and tortuous aorta, and pelvic prolapse due to disorganized and fragmented elastic fibers (14,15,35). Despite the wide spread effects of the absence of fibulin-4 or 5 on elastic fibers, fibulin-3 deficiency is not compensated for by fibulin-4 or 5. Unlike fibulin-4 or 5, fibulin-3 shows little interaction with elastic fiber components (17,18). Therefore, fibulin-3 is not likely to be a critical player in elastic fiber assembly. Rather, it may be an antagonist for ECM enzyme(s) as we hypothesized, and the elastic fiber defect in *Efemp1*$^{-/-}$ mice may be due to excessive degradation secondary to loss of fibulin-3's protective function.

General defects in collagen or elastic fibers can cause hernias, but they usually also lead to other systematic problems such as vascular and lung dysfunctions. For example, Marfan syndrome patients have skeletal, lung and vascular abnormalities resulting from microfibril and elastic fiber defects (36). Some collagen fiber defects lead to Ehlers-Danlos syndrome, which has skin and other pathological manifestations (37). Both Marfan syndrome and Ehlers-Danlos syndrome patients are at higher risk of developing inguinal hernias (38,39). It is unique that *Efemp1*$^{-/-}$ mice develop large inguinal hernias and other protrusions, but are devoid of obvious defects in other systems. Inguinal hernias commonly occur in humans without other systematic conditions and some families are genetically predisposed (40,41). Thus, our findings suggest that mutations or other defects in the *EFEMP1* gene could be one cause of inguinal hernias in humans.

A R345W mutation in the *EFEMP1* gene causes ML, an inherited form of macular degeneration characterized by sub-RPE deposits within or attached to Bruch's membrane. The lack of defects or deposits in Bruch's membrane characteristic of macular degeneration in *Efemp1*$^{-/-}$ mice suggests that loss of fibulin-3 function does not cause macular degeneration. The middle layer of Bruch's membrane is similar to fascia in the sense that it is an ultra thin layer of connective tissue containing collagen fibers, elastic fibers and other ECM components including proteoglycans (29). We did find that the elastic fibers of Bruch's membrane in *Efemp1*$^{-/-}$ mice were less intact than those in wild-type mice. This is in contrast to the phenotype of *Efemp1* knock-in mice harboring the R345W mutation which develops symptoms of macular degeneration but is otherwise normal (31,32). ML patients carrying the R345W mutation are not known to have other systemic symptoms (6). Thus, it is likely that the R345W mutation in the *EFEMP1* gene does not disrupt fibulin-3's normal function. Bruch's membrane is located between the RPE/photoreceptors and their blood supply in the choroid. In addition to acting as a support element and

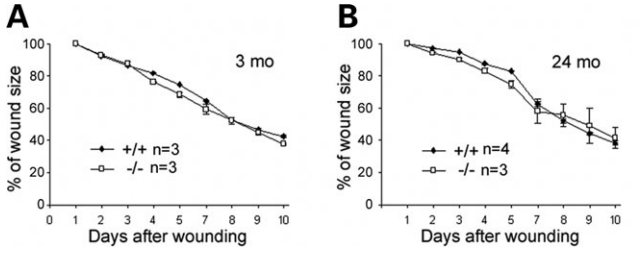

Figure 9. Normal wound healing in *Efemp1*$^{-/-}$ mice. Wound sizes were similar in wild-type and *Efemp1*$^{-/-}$ mice at 1–10 days after wounding in both 3 month-old (**A**) and 24 month-old mice (**B**). +/+, wild-type; −/−, *Efemp1*$^{-/-}$. Data are mean ± SD.

an attachment site for the RPE, it provides a semipermeable diffusion barrier through which metabolic exchange takes place (29). The R345W mutation may have an added detrimental effect that affects Bruch's membrane to a greater extent than other tissues to cause macular degeneration because of its strategic location and unique function. For example, mutant fibulin-3 may cause the formation of a structurally altered Bruch's membrane that induces an injury response from RPE cells by secreting excess basement membrane. This may in turn cause the formation of sub-RPE deposits and impair the diffusion property of Bruch's membrane.

In summary, the data presented in this study support a role for fibulin-3 in elastic fiber integrity in fascia connective tissues and in the regulation of aging. Our results underscore the function of fascia, a seemingly unobtrusive, but overwhelming abundant and extensive tissue. Based on our findings, we put forth a novel hypothesis, that fascia defects are an important but previously unrecognized contributor to aging. Further studies using the *Efemp1*$^{-/-}$ mouse model will therefore undoubtedly provide additional valuable information concerning the function of fibulin-3 both in the maintenance of elastic fiber integrity and in the role of fascia membranes in aging.

MATERIALS AND METHODS

Efemp1$^{-/-}$ mouse generation, breeding and maintenance

The mouse *Efemp1* gene was isolated from a genomic 129/SvJ mouse library. A replacement targeting vector was constructed using a 3.6 kb fragment from intron III and a 5 kb fragment from exon 5 to intron V of the gene as the 5′ and 3′ arms of homology, respectively (Fig. 1). Both fragments were subcloned into the vector PGKneolox2DTA. The targeting construct was linearized and electroporated into 129 Sv/J ES cells (Cell and Molecular Technologies, Inc.). Homologous recombination between the wild-type locus and the targeting vector resulted in the replacement of 1 kb of genomic DNA, including exon 4 and part of exon 5, with the 1.8 kb neo^{r} cassette. Recombinant clones were injected into C57BL/6 blastocysts to generate chimeras. Germline-transmitting chimeras were crossed two generations into BALB/c or C57BL/6 strains, so that the mice in this study were mixed inbred 129Sv/J-BALB/c or 129Sv/J-C57BL/6 mice. Heterozygotes determined by Southern blot analysis of tail DNA were inbred to yield *Efemp1*$^{-/-}$ homozygous mutants (Fig. 1).

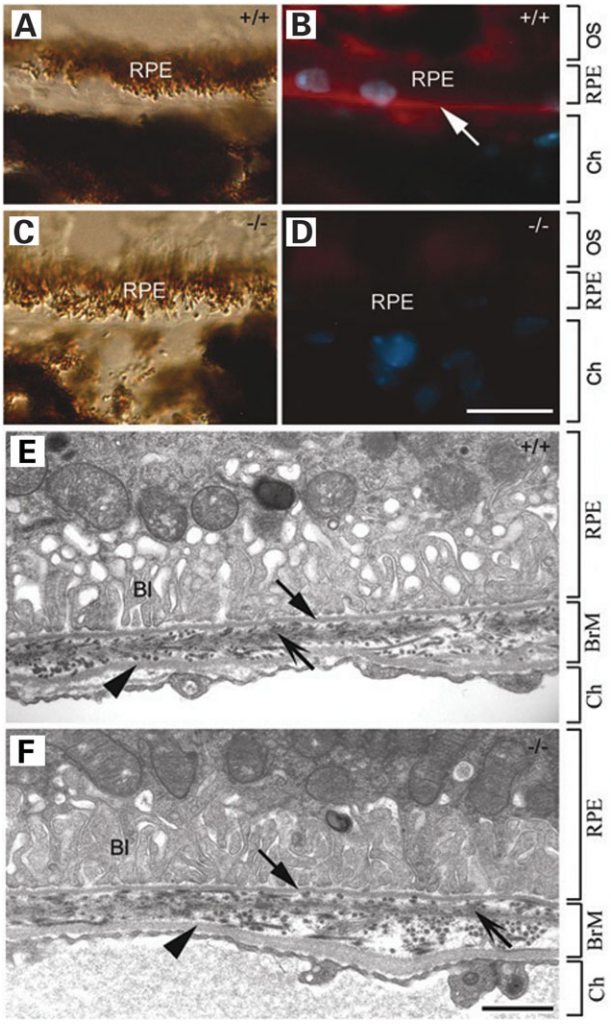

Figure 10. Immunofluorescence and electron microscopy of Bruch's membranes in wild-type and *Efemp1*$^{-/-}$ mice. (**A**) A differential interference contrast (DIC) image showing the RPE and Bruch's membrane area of an eye section from a 14 month-old wild-type mouse. (**B**) The immunofluorescence image of the same area as in (A). Note fibulin-3 staining (red) in Bruch's membrane (white arrow). RPE and choroidal cell nuclei were stained blue with DAPI. (**C**) A DIC image showing the RPE and Bruch's membrane area of an eye section from a 14 month-old *Efemp1*$^{-/-}$ mouse. (**D**) The immunofluorescence image of the same area as in (C). Note a lack of fibulin-3 staining in the *Efemp1*$^{-/-}$ mouse. (**E**and**F**) Electron microscopy of the Bruch's membrane area of 18 month-old wild-type (E) and *Efemp1*$^{-/-}$ (F) mice. Arrows indicating the basement membrane of the RPE; arrowheads indicating the basement membrane of the choroidal capillary endothelial cells; concave arrows indicating the elastic fiber layer of Bruch's membrane. OS, photoreceptor outer segments; Ch, choroid; BI, RPE basal infoldings; BrM, Bruch's membrane. Scale bars: 10 μm (A–D) and 1 μm (E and F).

Southern blot, RT–PCR and western blot

Southern blot analysis and RT–PCR were performed as previously described (16) to identify homologous recombinants and to confirm the absence of *Efemp1* mRNA expression in

homozygous mice. DNA was digested with BsrGI and BlpI and hybridized with an external probe corresponding to sequences outside of the homologous arm regions. Either a 5′ or 3′ primer set corresponding to mouse *Efemp1* cDNA sequence was used in the PCR reactions. 5′ primer set 5′-ATGTTGCAAACACTTTTCCTAAC-3′ and 5′-GGGTTTCT TCGGATGACAAAG-3′ generates a 428-bp fragment; and 3′ primer set 5′-CCACGAAACCCATGTCAAGA-3′ and 5′-AATGAAAATGGCCCCACTATTA-3′ generates a 418-bp fragment. *Fibulin-4* primers were used in the control.

For western blot, mice were sacrificed by CO_2 asphyxiation and immediately perfused with TBS (pH 7.45) to flush out the blood from tissues. Lung tissues were collected and homogenized in TBS (pH 7.45) containing 10 mM EDTA, 5 mM NEM and 2 mM PMSF. After centrifugation, the supernatants were collected and the total protein concentration was determined with a BCA assay (Pierce). Tissue extracts were separated on a 10% SDS-PAGE gel and western blotting was performed as previously described with a polyclonal anti-mouse fibulin-3 antibody (42).

Mouse reproductivity and longevity

Efemp1$^{-/-}$ mice were bred with wild-type or *Efemp1*$^{+/-}$ mice to determine their reproductivity. As controls, wild-type or *Efemp1*$^{+/-}$ mice were interbred. The number of litters and the number of pups in each litter were recorded (Supplementary Material, Table S1). The entire mouse colony was monitored for longevity over their lifespan. Mice that died of apparent non-natural causes (e.g. cage fight injuries, pan flood accidents) were excluded from the longevity data.

Analysis of mouse aging phenotypes

Mice were inspected visually for gross changes weekly. Littermates of wild-type, heterozygous, and homozygous mice were co-caged and inspected side by side. Autopsy analysis was performed after mice were sacrificed. Internal organs including liver, spleen, and kidney were removed and weighed. The calf muscles were isolated and weighed. Whole-body X-rays were performed for bone analysis using a micro CT system. Projection X-ray images were obtained at a voltage of 32 kVp and an anode current of 0.4 mA with 1 s acquisition.

Histological analysis

Mice were sacrificed by CO_2 asphyxiation and tissues were collected, fixed in 10% neutral-buffered formalin or 4% paraformaldehyde in 0.1 M phosphate buffer, pH 7.2, dehydrated, and embedded in paraffin. Sections of 10 μm were stained with hemotoxylin and eosin (H&E), for elastin using an elastin staining kit (Sigma), or for collagen using a Masson's trichrome stain kit (Diagnostic BioSystems) according to manufacture's instructions.

Spread preparations of fascia membranes were prepared as follows: fascia membranes were sampled from under the skin, abdominal wall and vesical ligaments associated with bladder and colorectum. Small pieces of membrane were spread out on glass slides and air-dried. The dried preparations were fixed with 4% paraformaldehyde and processed for staining using H&E, an elastin staining kit, or a Masson's trichrome stain kit.

For transmission electron microscopy of the eye, lung and aorta, tissues were fixed in half-strength Karnovsky's fixative (2.5% gluteraldehyde and 2% paraformaldehyde in 0.1 M cacodylate buffer, pH 7.2) overnight and then postfixed with 1% osmium tetroxide, stained in 2% tannic acid, dehydrated in a graded series of alcohols and embedded in epoxy resin. Thin sections were cut on a Reichert Ultracut microtome and stained with uranyl acetate and lead citrate. Samples were examined and photographed using a Philips CM-12 electron microscope equipped with an AMT CCD camera (Advanced Microscopy Techniques Corp., Danvers, MA, USA) and AMTV542 software. For transmission electron microscopy of the dermis, strips of skin were trimmed into 1 mm^3 pieces and fixed with 3% glutaraldehyde in 0.1 M sodium cacodylate (pH 7.4) overnight at 4°C, sequentially treated with osmium tetroxide, tannic acid and uranyl acetate, then dehydrated and embedded in Epon as previously described (43). Thin sections (60 nm) were counterstained with methanolic uranyl acetate and lead citrate, and viewed using a Tecnai 12 transmission electron microscope at 120 kV. The images were digitally captured.

Immunofluorescence

Mouse tissues fixed in 4% paraformaldehyde were cryoprotected in 30% sucrose in PBS and embedded in OCT at −20°C. Immunofluorescence staining of 10 μm cryosections was performed as previously described (17) using an affinity purified polyclonal anti-mouse fibulin-3 antibody. Cell nuclei were stained with 4′,6-diamidino-2-phenylindole (DAPI). Stained sections were examined and photographed using a Nikon E600 microscope equipped with a CCD camera and ACTII software (Nikon Inc.).

Wound healing analysis

Full-thickness wounds were induced as described previously (44) with modification. Age-matched *Efemp1*$^{+/+}$ and *Efemp1*$^{-/-}$ mice were anesthetized with Avertin (250 mg/kg). For the duration of each wound-healing experiment acetaminophen (Children's Tylenol) was added to the drinking water at 1 mg/ml and sulfamethoxazole/trimethoprim oral suspension was added at 1 ml/150 ml. Circular wounds were generated using a 3-mm biopsy punch in the center of the back after shaving using an electric razor. Wounds were monitored over a period of 10 days for closure and wound diameters were measured per time point (1, 2, 3, 4, 5, 7, 8, 9 and 10 days).

Hair regrowth assay

Age-matched *Efemp1*$^{+/+}$ and *Efemp1*$^{-/-}$ mice were shaved on their lower back using an electric razor and monitored for hair regrowing for 25 days. Hair regrowth was measured as described previously (45). Briefly, an approximately 2-cm^2 area was shaved in each mouse. Hair regrowth was defined as the first appearance of hair and was scored using a transparent screen with grids dividing the area into eight equal portions.

SUPPLEMENTARY MATERIAL

Supplementary Material is available at HMG Online.

ACKNOWLEDGEMENTS

We thank Brett Stanton for technical assistance; Peggy McCuskey for assistance with electron microscopy; and Dr Philippe Soriano for providing the PGKneolox2DTA vector.

Conflict of Interest statement. None declared.

FUNDING

This work was supported by National Institutes of Health/NEI grants EY13847 (LYM) and EY13160 (ADM), the Macular Vision Research Foundation (ADM), Synfrämjandet and the Swedish Research Council (BB), and a Career Development Award (LYM) and an unrestricted grant from Research to Prevent Blindness to the Department of Ophthalmology and Vision Science at the University of Arizona. ECD is a Canada Research Chair supported by a CIHR operating grant MOP-57663.

REFERENCES

1. Argraves, W.S., Greene, L.M., Cooley, M.A. and Gallagher, W.M. (2003) Fibulins: physiological and disease perspectives. *EMBO Rep.*, **4**, 1127–1131.
2. Chu, M.L. and Tsuda, T. (2004) Fibulins in development and heritable disease. *Birth Defects Res. Part C Embryo Today*, **72**, 25–36.
3. Gallagher, W.M., Currid, C.A. and Whelan, L.C. (2005) Fibulins and cancer: friend or foe? *Trends Mol. Med.*, **11**, 336–340.
4. Timpl, R., Sasaki, T., Kostka, G. and Chu, M.L. (2003) Fibulins: a versatile family of extracellular matrix proteins. *Nat. Rev. Mol. Cell. Biol.*, **4**, 479–489.
5. Stone, E.M., Lotery, A.J., Munier, F.L., Heon, E., Piguet, B., Guymer, R.H., Vandenburgh, K., Cousin, P., Nishimura, D., Swiderski, R.E. *et al.* (1999) A single EFEMP1 mutation associated with both Malattia Leventinese and Doyne honeycomb retinal dystrophy. *Nat. Genet.*, **22**, 199–202.
6. Marmorstein, L. (2004) Association of EFEMP1 with Malattia Leventinese and age-related macular degeneration: a mini-review. *Ophthalmic Genet.*, **25**, 219–226.
7. Piguet, B., Haimovici, R. and Bird, A.C. (1995) Dominantly inherited drusen represent more than one disorder: a historical review. *Eye*, **9**, 34–41.
8. Bressler, N.M., Bressler, S.B. and Fine, S.L. (1988) Age-related macular degeneration. *Surv. Ophthalmol.*, **32**, 375–413.
9. Stone, E.M., Braun, T.A., Russell, S.R., Kuehn, M.H., Lotery, A.J., Moore, P.A., Eastman, C.G., Casavant, T.L. and Sheffield, V.C. (2004) Missense variations in the fibulin 5 gene and age-related macular degeneration. *N. Engl. J. Med.*, **351**, 346–353.
10. Hucthagowder, V., Sausgruber, N., Kim, K.H., Angle, B., Marmorstein, L.Y. and Urban, Z. (2006) Fibulin-4: a novel gene for an autosomal recessive cutis laxa syndrome. *Am. J. Hum. Genet.*, **78**, 1075–1080.
11. Loeys, B., Van Maldergem, L., Mortier, G., Coucke, P., Gerniers, S., Naeyaert, J.M. and De Paepe, A. (2002) Homozygosity for a missense mutation in fibulin-5 (FBLN5) results in a severe form of cutis laxa. *Hum. Mol. Genet.*, **11**, 2113–2118.
12. Markova, D., Zou, Y., Ringpfeil, F., Sasaki, T., Kostka, G., Timpl, R., Uitto, J. and Chu, M.L. (2003) Genetic heterogeneity of cutis laxa: a heterozygous tandem duplication within the fibulin-5 (FBLN5) gene. *Am. J. Hum. Genet.*, **72**, 998–1004.
13. Xiang, Y., Sekine, T., Nakamura, H., Imajoh-Ohmi, S., Fukuda, H., Yudoh, K., Masuko-Hongo, K., Nishioka, K. and Kato, T. (2006) Fibulin-4 is a target of autoimmunity predominantly in patients with osteoarthritis. *J. Immunol.*, **176**, 3196–3204.
14. Nakamura, T., Lozano, P.R., Ikeda, Y., Iwanaga, Y., Hinek, A., Minamisawa, S., Cheng, C.F., Kobuke, K., Dalton, N., Takada, Y. *et al.* (2002) Fibulin-5/DANCE is essential for elastogenesis in vivo. *Nature*, **415**, 171–175.
15. Yanagisawa, H., Davis, E.C., Starcher, B.C., Ouchi, T., Yanagisawa, M., Richardson, J.A. and Olson, E.N. (2002) Fibulin-5 is an elastin-binding protein essential for elastic fibre development in vivo. *Nature*, **415**, 168–171.
16. McLaughlin, P.J., Chen, Q., Horiguchi, M., Starcher, B.C., Stanton, J.B., Broekelmann, T.J., Marmorstein, A.D., McKay, B., Mecham, R., Nakamura, T. *et al.* (2006) Targeted disruption of fibulin-4 abolishes elastogenesis and causes perinatal lethality in mice. *Mol. Cell. Biol.*, **26**, 1700–1709.
17. Kobayashi, N., Kostka, G., Garbe, J.H., Keene, D.R., Bachinger, H.P., Hanisch, F.G., Markova, D., Tsuda, T., Timpl, R., Chu, M.L. *et al.* (2007) A comparative analysis of the fibulin protein family. Biochemical characterization, binding interactions, and tissue localization. *J. Biol. Chem.*, **282**, 11805–11816.
18. El-Hallous, E., Sasaki, T., Hubmacher, D., Getie, M., Tiedemann, K., Brinckmann, J., Batge, B., Davis, E.C. and Reinhardt, D.P. (2007) Fibrillin-1 interactions with fibulins depend on the first hybrid domain and provide an adaptor function to tropoelastin. *J. Biol. Chem.*, **282**, 8935–8946.
19. Lecka-Czernik, B., Lumpkin, C.K., Jr and Goldstein, S. (1995) An overexpressed gene transcript in senescent and quiescent human fibroblasts encoding a novel protein in the epidermal growth factor-like repeat family stimulates DNA synthesis. *Mol. Cell. Biol.*, **15**, 120–128.
20. Giltay, R., Timpl, R. and Kostka, G. (1999) Sequence, recombinant expression and tissue localization of two novel extracellular matrix proteins, fibulin-3 and fibulin-4. *Matrix. Biol.*, **18**, 469–480.
21. Ehlermann, J., Weber, S., Pfisterer, P. and Schorle, H. (2003) Cloning, expression and characterization of the murine Efemp1, a gene mutated in Doyne-Honeycomb retinal dystrophy. *Gene. Expr. Patterns*, **3**, 441–447.
22. Albig, A.R., Neil, J.R. and Schiemann, W.P. (2006) Fibulins 3 and 5 antagonize tumor angiogenesis in vivo. *Cancer Res.*, **66**, 2621–2629.
23. Marmorstein, L.Y., Munier, F.L., Arsenijevic, Y., Schorderet, D.F., McLaughlin, P.J., Chung, D., Traboulsi, E. and Marmorstein, A.D. (2002) Aberrant accumulation of EFEMP1 underlies drusen formation in Malattia Leventinese and age-related macular degeneration. *Proc. Natl. Acad. Sci. USA*, **99**, 13067–13072.
24. Salmons, S. (1995) Muscle. In Bannister, L.H., Berry, M.M., Collins, P., Dyson, M., Dussek, J.E. and Ferguson, M.W.J. (eds), *Gray's Anatomy*, 38th edn. Churchill Livingstone, Edinburgh.
25. Arking, R. (1998) *Biology of Aging*, 2nd edn.Sinauer, Sunderland, Massachusetts.
26. Chuttani, A. and Gilchrest, B.A. (1995) Aging. In Masoro, E.J. (ed.), *Handbook of Physiology*. Oxford University Press, New York, pp. 309–324.
27. Takeda, T., Hosokawa, M., Takeshita, S., Irino, M., Higuchi, K., Matsushita, T., Tomita, Y., Yasuhira, K., Hamamoto, H., Shimizu, K. *et al.* (1981) A new murine model of accelerated senescence. *Mech. Ageing Dev.*, **17**, 183–194.
28. Ashcroft, G.S., Mills, S.J. and Ashworth, J.J. (2002) Ageing and wound healing. *Biogerontology*, **3**, 337–345.
29. Guyer, D.R., Schachat, A.P. and Green, W.R. (2001) The choroids: structural consideration. In Ryan, S.J. (ed.), *Retina*. Mosby, St. Louis, p. 29.
30. Marmorstein, A.D. and Marmorstein, L.Y. (2007) The challenge of modeling macular degeneration in mice. *Trends Genet.*, **23**, 225–231.
31. Fu, L., Garland, D., Yang, Z., Shukla, D., Rajendran, A., Pearson, E., Stone, E.M., Zhang, K. and Pierce, E.A. (2007) The R345W mutation in EFEMP1 is pathogenic, and causes AMD-like deposits in mice. *Hum. Mol. Genet.*, doi:10.1093/hmg/ddm198.
32. Marmorstein, L.Y., McLaughlin, P.J., Peachey, N.S., Sasaki, T. and Marmorstein, A.D. (2007) Formation and progression of sub-retinal pigment epithelium deposits in Efemp1 mutation knock-in mice: a model for the early pathogenic course of macular degeneration. *Hum. Mol. Genet.*, doi:10.1093/hmg/ddm199.
33. Klenotic, P.A., Munier, F.L., Marmorstein, L.Y. and Anand-Apte, B. (2004) Tissue inhibitor of metalloproteinases-3 (TIMP-3) is a binding partner of epithelial growth factor-containing fibulin-like extracellular matrix protein 1 (EFEMP1). Implications for macular degenerations. *J. Biol. Chem.*, **279**, 30469–30473.

34. Van den Steen, P.E., Van Aelst, I., Starckx, S., Maskos, K., Opdenakker, G. and Pagenstecher, A. (2006) Matrix metalloproteinases, tissue inhibitors of MMPs and TACE in experimental cerebral malaria. *Lab. Invest.*, **86**, 873–888.
35. Drewes, P.G., Yanagisawa, H., Starcher, B., Hornstra, I., Csiszar, K., Marinis, S.I., Keller, P. and Word, R.A. (2007) Pelvic organ prolapse in fibulin-5 knockout mice: pregnancy-induced changes in elastic fiber homeostasis in mouse vagina. *Am. J. Pathol.*, **170**, 578–589.
36. von Kodolitsch, Y. and Robinson, P.N. (2007) Marfan syndrome: an update of genetics, medical and surgical management. *Heart*, **93**, 755–760.
37. Mao, J.R. and Bristow, J. (2001) The Ehlers-Danlos syndrome: on beyond collagens. *J. Clin. Invest.*, **107**, 1063–1069.
38. Kashyap, A.S., Anand, K.P. and Kashyap, S. (2004) Inguinal and incisional hernias. *Lancet.*, **363**, 84.
39. Liem, M.S., van der Graaf, Y., Beemer, F.A. and van Vroonhoven, T.J. (1997) Increased risk for inguinal hernia in patients with Ehlers-Danlos syndrome. *Surgery*, **122**, 114–115.
40. Lau, H., Fang, C., Yuen, W.K. and Patil, N.G. (2007) Risk factors for inguinal hernia in adult males: a case-control study. *Surgery*, **141**, 262–266.
41. Ruhl, C.E. and Everhart, J.E. (2007) Risk factors for inguinal hernia among adults in the US population. *Am. J. Epidemiol.*, **165**, 1154–1161.
42. Marmorstein, L.Y., McLaughlin, P.J., Stanton, J.B., Yan, L., Crabb, J.W. and Marmorstein, A.D. (2002) Bestrophin interacts physically and functionally with protein phosphatase 2A. *J. Biol. Chem.*, **277**, 30591–30597.
43. Davis, E.C. (1993) Smooth muscle cell to elastic lamina connections in developing mouse aorta. Role in aortic medial organization. *Lab. Invest.*, **68**, 89–99.
44. Wojcik, S.M., Bundman, D.S. and Roop, D.R. (2000) Delayed wound healing in keratin 6a knockout mice. *Mol. Cell Biol.*, **20**, 5248–5255.
45. Harrison, D.E. and Archer, J.R. (1988) Biomarkers of aging: tissue markers. Future research needs, strategies, directions and priorities. *Exp. Gerontol.*, **23**, 309–325.